Characteristics of climatic variation from the perspective of “the Silk Road Economic Belt”

Anfeng Qiang[a], Ni Wang[a,*], Jiancang Xie[a], Jiahua Wei[b,c], Xia Wei[a]

[a] State Key Laboratory of Eco-Hydrologic Engineering in Northwest Arid Region of China, Xi'an University of Technology, Xi'an 710048, China

[b] State Key Laboratory of Plateau Ecology and Agriculture, Qinghai University, Xining 810016, China

[c] State Key Laboratory of Hydroscience and Engineering, Tsinghua University, Beijing 100084, China

Corresponding author.E-mail: wangni @xaut.edu.cn

Abstract

The variance tendency of climatic and spatial-temporal equilibrium characteristics of major cities along the SREB were systematically described through moving mean method, Kriging interpolation method, Bernaola-Galvan algorithm and correlation analysis based on monthly scale data of global weather stations released by the National Climatic Data Center website since 1951. Some conclusions cloud be drawn: (1) The precipitation showed a downward trend in other districts with significant seasonal differences except the Europe. The annual precipitation was “N” type distribution in Central Asia, while showed an "inverted V" and a "positive V" distribution in the East Asia and West Asia respectively, and the precipitation change was relatively gentle in Europe. The dominant factors affecting climate were different in different districts. (2) The temperature continued to increase in all districts and the seasonal temperature presented unimodal distribution, the alternation of drying and wetting was obvious in each districts as well as the temperature was complex and changeable in Europe. (3) The mutation point of temperature was detected by using Bernaola-Galvan algorithm in all districts, but the timing of the mutation was not synchronous and the mutation point of precipitation was not detected except in Europe. (4) The precipitation was decreasing from west to east in space, and the temperature showed the morphological distribution characteristics of of low in the middle but high on both sides. (5) The change of temperature were more sensitive than precipitation, the precipitation in Central Asia was inversely correlated with other districts, however, there was a high positive correlation between temperature in all districts. The inversely correlation between temperature and precipitation was the most significant in Central Asia.

Keywords: the Silk Road Economic Belt, climatic variation, spatial-temporal distribution, water resources

1 Introduction

The grand economic vision of the Belt and Road (BR) was proposed and promoted by China in 2013, many countries and international organizations had taken an active part in the activities so that they committed to building a community of shared interests, shared future and shared responsibilities featuring political mutual trust, economic integration and cultural inclusiveness. The participating countries and China had achieved Effective and practical achievements in many fields and the related researches have been deepened continuously on the development road of BR. Water resources pressure and water disasters were common challenges facing the world, food security is one of the ten major changes in the international economic landscape in the next 15 years, food security situation was grim in some regions and the problem of regional

imbalances were prominent. This problem that the water supply, demand allocation and sustainable utilization must be solved to ensure global food security. Water resources cooperation was divided into water resources policy communication, infrastructure cooperation, water disaster prevention and control, technological and humanistic exchanges, etc according to the important contents of the "five links" of BR and the characteristics of water resources. Therefore, water resources played an important supporting role in promoting BR construction. After the full implementation of the BR strategy, when China's water resources only showed the fundamental characteristics of comprehensive and coordinated development can provide favorable water resources guarantee for the development of BR. Thus, the comprehensive and coordinated economic development between China and participating countries can be further promoted to minimize the differences in regional development (Jiang 2019).

At present, there was a lack of research achievements about BR water resources, which was mainly focused on macroscopic description of water resources theory or single water security problem, etc. (Jiang 2019; Tan et al. 2016). Water resources environmental problems along the economic belt were prominent and its were payed closely concern to scholars, who would focus their research perspective on the methods and quantitative analysis. Tan et al. (2016) estimated the water efficiency and made cluster analysis using the Stochastic Frontier Analysis (SFA) method of the Silk Road Economic Belt (SREB) from different perspectives, she had putted forward the targeted policy suggestions that its played an important role in the green construction of the new SREB. Water-use efficiency in the core area of China's SREB had been significantly improved in the overall goal for “the Measures for Assessment of Implementation of the Strictest Management System for Water Resources” in the past 22 years, but there was still a gap with developed countries (Yan et al. 2018), uneven distribution degree of water resources was grievous in Central Asia (CA). Lin (2015) discussed the integrated management of water resources about five countries in CA. Therefore, water resource management still became one of the important resource factors restricting the strategic layout of BR (Zhang 2015; OECD 2015).

How to made a breakthrough in water resources allocation in terms of management, it was necessary to clearly define the precipitation (*P*) distribution and regularity of climate change in every country. Analyzing the natural endowment and utilization of water resources along the countries was conducive to promoting scientific development and construction of BR from the perspective of water resources development and utilization (Yang et al. 2019). The climate change had a preliminary basic research in the Maritime Silk Road Economic Belt (MSREB) in the 21st century at present (Qi & Cai 2017; Qi & Cai 2017; Zhou et al. 2018; Zhen et al. 2019), Han et al. (2018) simulated and evaluated the variation of extreme values associated with the temperature (*T*) and *P* using the coupling model CMIP5 in the BR district in the middle and late 21st century. Dong et al. (2018) evaluated the property of climate simulations using the same model and predicted future changes in the key BR districts under RCP2.6, RCP4.5 and RCP8.5, the most significant warming was expected to occur in Kazakhstan (KAZ) and the northern part of the BR district, the increase of regional warming was more significant under the scenario of high-emissions. Peng et al. (2018) used the atmospheric model CAM5.1 to analyze human contribution rate to the summer *P* in CA from 1961 to 2013 and found that anthropogenic warming increased the specific humidity of the whole CA and the *P* in the climatically rising region of eastern CA. Wang et al. (2018) used Mann-Kendall (M-K) rank-order correlation test and wavelet analysis to analyze the spatial-temporal equilibrium characteristics of *P* in the main water resources areas of CA. Districts along the BR had fragile ecological environment, concentrated agricultural farmland and frequent drought disasters. Bai et al. (2017) had analyzed the drought region differentiation characteristics using the drought model of anomaly percentage of *P* and Breaks For Additive Seasonal and Trend (BFAST) algorithm based on the *P* data of TRMM in the BR district. Xu (2016) systematically elaborated the variation trend and spatial distribution characteristics of *T* and *P* in major countries of SREB from 1980 to 2014, but the research mainly focused on South Asia (SA) and southeast Asia. Based on the above summary, we found that there was almost

blank on climate change in the whole SREB district, therefore, it is of great importance to study the distribution of water resources and climate change of SREB in order to reveal the variation regularity characteristic of *P* under changing environment. It will provide a basis for further study on agricultural production and natural disasters in the future, also help to clarify the situation of countries in climate change and lay the scientific foundation for cooperation and policy needs of BR.

2 Study area and division

2.1 SREB profile and socioeconomic

The proposed concept of SREB was of great significance to dredge the overland trade between Europe (E) and Asia again, strengthen the economic and trade relations between E and Asian countries, and promote regional economic integration. SREB started from China in the east and passed through the CA, Asia and SA across the North, Middle and South, then passed by the Caspian Sea, the Black Sea, the Mediterranean Coast and the Arabian Peninsula to the west to E and North America. The major cities of SREB passed through in China were Xi'an, Lanzhou and Urumqi, the road broke the seaway in the Baltic Ocean and the Pacific Ocean and formed a transportation network connecting East Asia (EA), West Asia (WA) and South Asia (SA), the E was divided into East Europe (EE), West Europe (WE), South Europe (SE) and Central Europe (CE). Fig. 1 for the research area.

Three line of SREB draw the outline of economic belt, the national industry chain will benefit from the perspective of economic geography that the scope was not limited to the countries along the routes, but also included North America, continental E and southeast Asia. It covered about 2.175 billion people, accounting for 30.87% of the world's population, and the scale of the total economy was about $16 trillion, accounting for 22.1% of the world's total. The economies directly involved in SREB accounted for a large proportion of international trade and outward foreign direct investment (OFDI) in the world. Moreover, the economies covered were highly complementary in economic structure, the agriculture represented by CA, the manufacturing represented by EA and CE as well as the scarce economies represented by other countries. Therefore, SREB had an important significance in promoting regional integration and economic development.

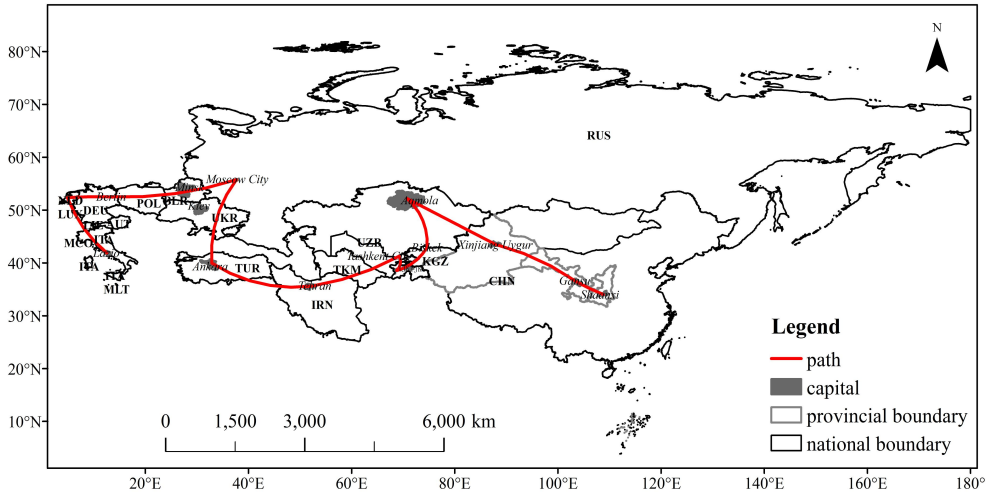

Fig.1. Demonstration area of the SREB (the thick red line represents the path of SREB)

2.2 SREB main water area and subarea

The main water resources areas of BR involved 12 provinces (cities and districts) and 61 tertiary subarea of water resources, with a total area of 3.174×10^6 km^2. There were spatial differences in water resources conditions and

carrying capacity indexes (Zuo et al. 2017). The main water resources areas of SREB were divided into 7 areas, 3 Asian areas and 4 European areas based on the main route taking into account the water systems and administrative units along the line, natural geography and water resource differences. The main water resources areas were the largest in EE and the least in CA (Table 1). The BR water problem could be summarized into 6 aspects, such as flood, drought, shortage, pollution, uneven distribution and inadequate water supply (Zuo et al. 2018). Water problems, the difficulties and solutions were different in different areas. Water resources cooperation of BR was confront with various problems, such as diverse infrastructure, complex trans-boundary river relations and social and cultural risks (Li et al. 2018).

Table 1 Water resources division and water resources quantity of the SREB (Zuo et al. 2018; Zuo et al. 2018)

Geographic position	First-level area of main water resources	Total water resources /billion m^3	Proportion/%	Involving state	Water problems
Asia	EA	28000	29.86	Xi'an Lanzhou Urumqi	Floods, droughts, shortages, pollution, uneven distribution and inadequate water supply
	WA	3545	3.78	Iran (IRN) Turkey (TUR)	Drought, shortage, pollution, uneven distribution and inadequate water supply
	CA	2276	2.43	Kazakhstan (KAZ) Kyrgyzstan (KYG) Tajikistan (TJR) Uzbekistan (UZB)	Drought, shortage, pollution, uneven distribution and inadequate water supply
E	EE	45829	48.88	Russia (RUS)	Inadequate water supply
	CE	3818	4.07	Germany (GER)	Floods, droughts, shortages and inadequate water supply
	WE	3203	3.41	Netherlands (NLD)	Shortages
	SE	7096	7.57	Italy (ITA)	Floods and inadequate water supply

3 Data and methods

3.1 Data source

This paper utilized global climate data sets (http://www.ncdc.noaa.gov/oa/ncdc.html) provided by the National Environmental Satellite Data Service (NESDIS), part of National Oceanic and Atmospheric Administration (NOAA), the National Climatic Data Center website (NCDC), the data set that the *P* and *T* data of SREB representing cities from 1951 to 2018 was selected for research. Detailed information was shown in Table 2 and the time series was not uniform. NCDC, one of the world's most prestigious meteorological data service center, operates and maintains the world's largest meteorological data system and is also responsible for the global weather data sharing service and climate change research, which has formed a complete set of satellite climate data product business system. It is characterized by fast updating speed, complete station data and high quality of meteorological data products. The involved fields mainly cover the geophysics, marine environment, air quality and water resources management, etc.

Table 2 Statistical table of *P*-*T* of the SREB in recent 60 years

Station	*P*/mm			*T*/°C		
	Average	Max\Min	Amplitude /a	Average	Max\Min	Amplitude /10a
Xi'an (1951-2008)	572.6	902.7(1983)\312.4(1995)	***-1.37***	14.3	16.1(2007)\12.9(2006)	0.31
Lanzhou (1951-2008)	312.2	546.4(1978)\158.0(2005)	***-0.88***	10.3	12.3(1998)\8.6(2005)	0.28
Urumqi (1951-2012)	268.8	419.6(2007)\131.3(1974)	1.42	7.4	9.3(1997)\4.0(1952)	0.39
KAZ (1951-2005)	***192.1***	348.0(1958)\87.4(1991)	***-0.90***	**4.7**	8.4(1955)\2.2(1972)	0.32
KYG (1951-1997)	372.0	672.3(1987)\300.0(1986)	0.55	10.4	12.2(1983)\7.5(1967)	0.33

TJR (1951-1996)	666.9	996.2(1969)\385.6(1995)	***-2.62***	15.2	16.9\(1988)13.0(1972)	0.24
UZB (1951-2017)	435.1	802.4(1969)\233.2(1995)	0.64	14.9	17.1(2016)\12.6(1972)	0.30
IRN (2000-2018)	233.7	447.3(2010)\99.3(2001)	2.01		Missing	
TUR (2006-2017)	550.9	821.4(2009)\393.7(2017)	***-2.43***		Missing	
RUS (1951-2017)	686.6	890.5(2013)\397.0(1964)	1.97	5.5	7.4(2008)\3.1(1956)	0.35
GER (1951-2018)	578.4	832.4(2007)\376.2(2018)	***-0.27***	9.7	11.7 (2018)\7.9(1996)	0.25
NLD (1951-2005)	***893.8***	1267.7(1999)\565.4(1976)	1.48		Missing	
ITA (1951-2009)	758.8	1123.7(2004)\370.8(1952)	2.82	**15.5**	17.1(2000)\14.2(1980)	0.09

3.2 Research methods

3.2.1 Moving average method

The moving average method used the recursive form to process non-stationary data quickly and in real-time, which could filter out the random errors of frequent fluctuations and showed the smooth change trend. At the same time, the variation process of random error could also be obtained to estimate its statistical characteristic quantity. The moving average method had a good inhibitory effect on periodic interference and had a high smoothness (Pei 2001). The selection of moving average method parameters would directly affect the smoothing effect of data, we usually chose reasonable parameters according to the changing mechanism of dynamic testing process and the changing state of testing data. The paper were smooth-processing the *P-T* curves in different regions of SREB in 1, 3 and 5 years respectively.

3.2.2 Kriging

The Kriging interpolation method was a specific sliding weighted average method based on the theory of variation function and structural analysis to carry out unbiased optimal estimation of variables in a finite region (Li et al. 2011), which was widely used in meteorology, hydrology and other fields (Xu et al. 2019). Kriging interpolation method, a spatial analysis tool in ArcGIS, was used to conduct spatial interpolation analysis on meteorological elements of SREB and analyzed its spatial characteristics of climate change.

3.2.3 B-G

B-G algorithm divided non-stationary time series into the time series with different-means and independently stationary based on *t* test, which overcome the disadvantages of previous detection methods for non-stationary time series. In addition, B-G adopted the method of dividing into two parts through multiple iterations in the process of segmentation, which greatly reduced the calculated quantities and had a stronger usability. It was an effective method for dealing with nonlinear and non-stationary time series, which was feasible and advantageous in hydrological time series (Wang et al. 2009). The heuristic segmentation method required the minimum segmentation scale $l_0 \geq 25$, and the length of the climate time series of the SREB was greater than 25 except IRN and TUR. The variation of precipitation and temperature could be analyzed by b-g method. The variation of *P* and *T* could be analyzed by B-G method, the Mann-Kendall (M-K) method was adopted to test the variation time if the variation didn't satisfy the B-G algorithm. References for the detailed calculation process (Ma et al. 2018; Qiang et al. 2018).

4 Results and discussion

4.1 Time variation characteristic of *P-T*

4.1.1 Interannual variation

Time series variation trend of cumulative climatic anomaly curve were showed in Fig. 2 and Fig. 3 in SREB district over the past 60 years, the 1-year, 3-year, and 5-year moving were chosen to represent the climatic variation of the short, medium, and long term, respectively. The average value, extremum value and

amplification of the *P* and *T* were listed in Table 2. The positive and negative extremum of cumulative anomaly was regard as the mutational point, and the change of cumulative anomaly curve could directly judge the sequence fluctuation.

The *P* showed a downward trend in EA except Urumqi and the *P* of the multi-year average (*P* = 379.1 mm) showed downward trend, the maximum and minimum values in 1958 and 1997 were 556.2 mm and 252.6 mm, respectively. Urumqi was a partial multi-stage after 1974 and the values of *P* and *T* in Xi'an were higher than those in Lanzhou, but the variation trends of the two places were basically the same (Fig. 3). The period of *P* could be divided into four stages (partial multi-stage: 1951-1964, 1983-2007; partial less-stage: 1965-1982, 2007-2012) and the sequence of *T* could be divided into two stages (1951-1988, 1989-2008) in EA. In general, the climate transformed from cold-wet to cold-dry before 1988 and showed a trend of warm-dry after 1988 in EA (Fig. 2). The conclusion was consistent with the research results of Xu (2016), some studies had shown that the warming and drying trend was related to the enhanced greenhouse effect in China in recent years (Zhao & Xu 2003; Shi et al. 2003).

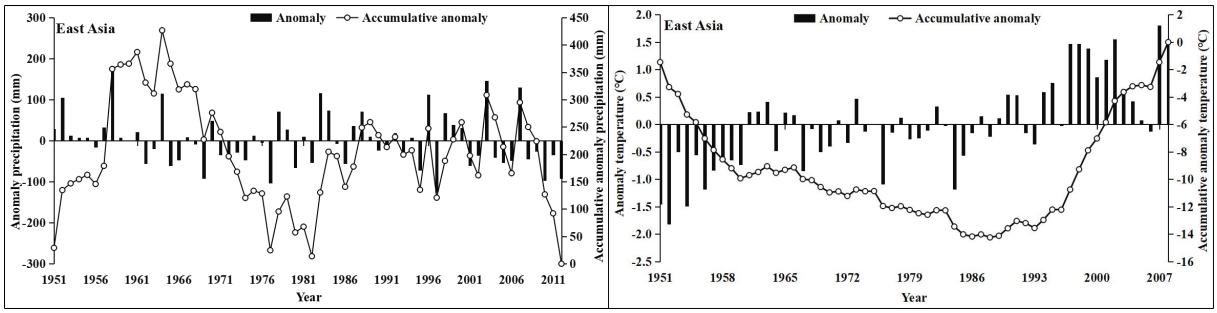

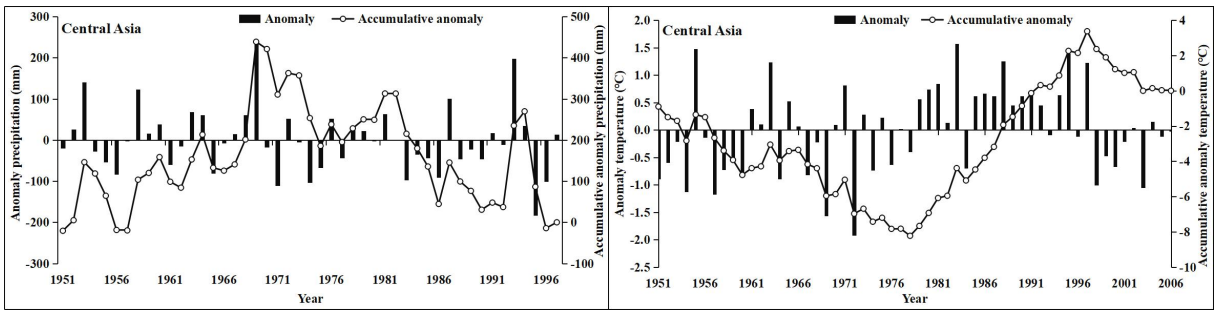

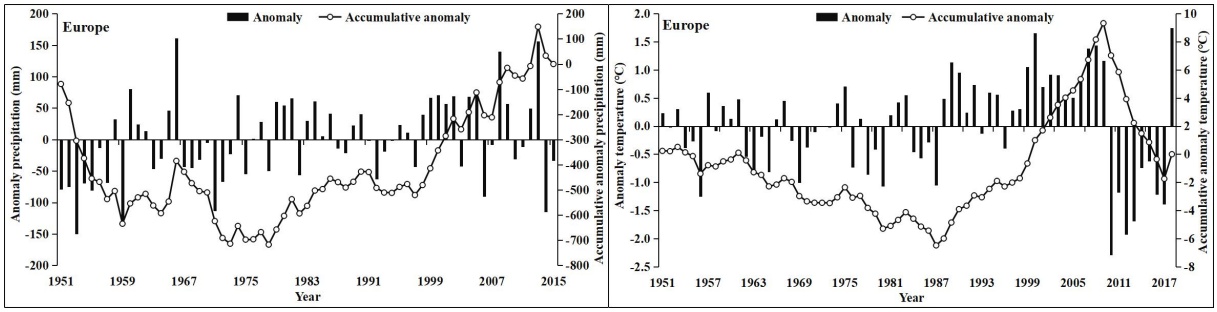

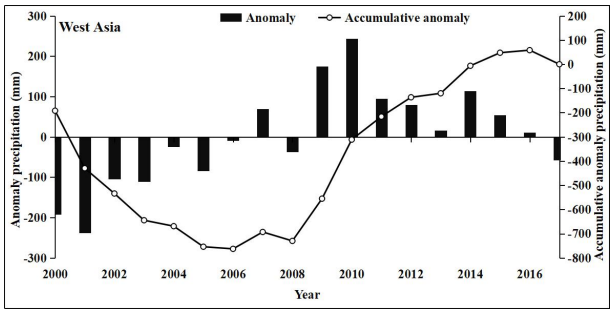

Fig.2. The annual variation of anomaly (left vertical axis) and cumulative anomaly (right vertical axis) of *P*-*T* in the SREB after 1951 (the time series was shorter in WA).

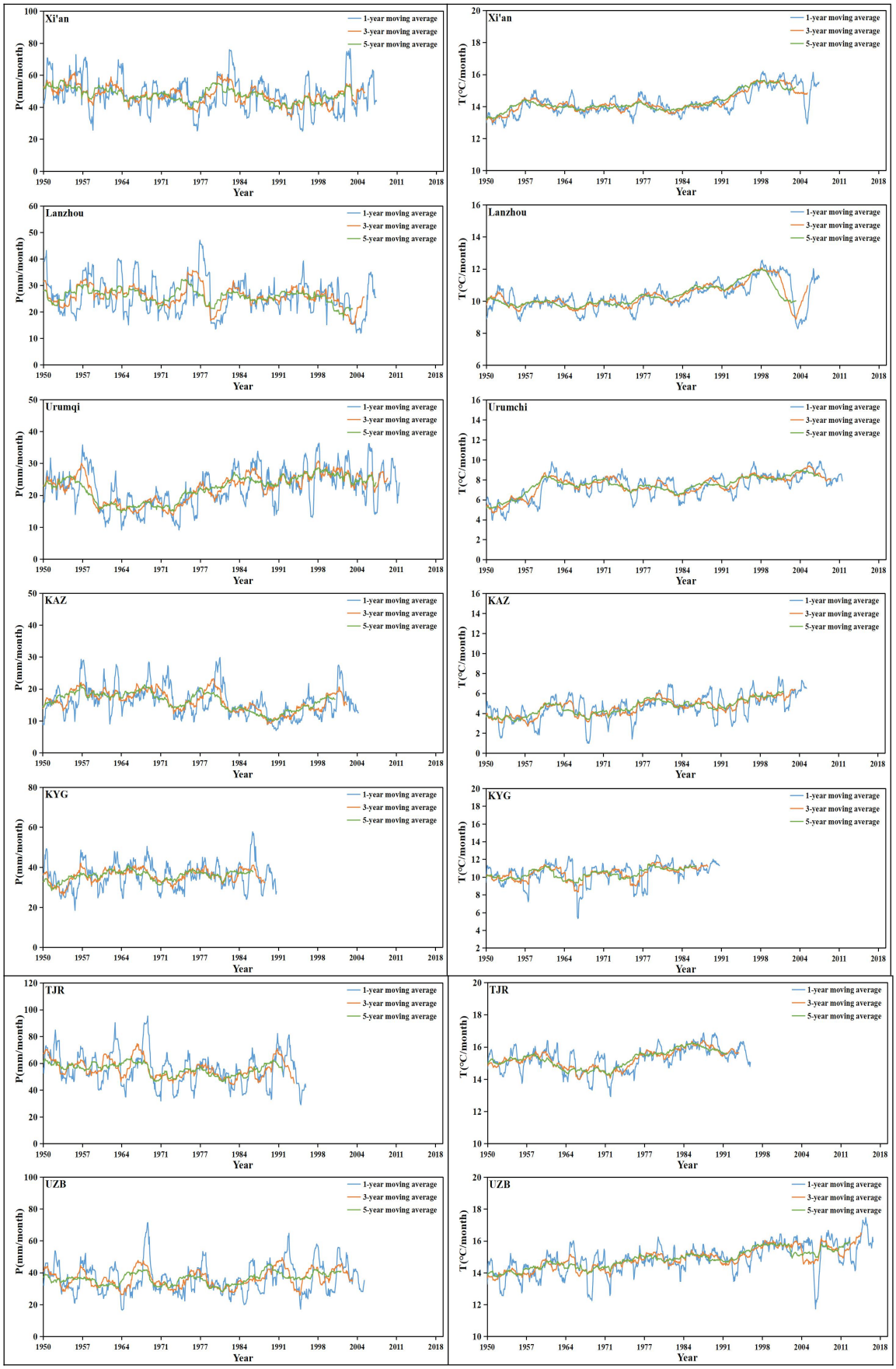

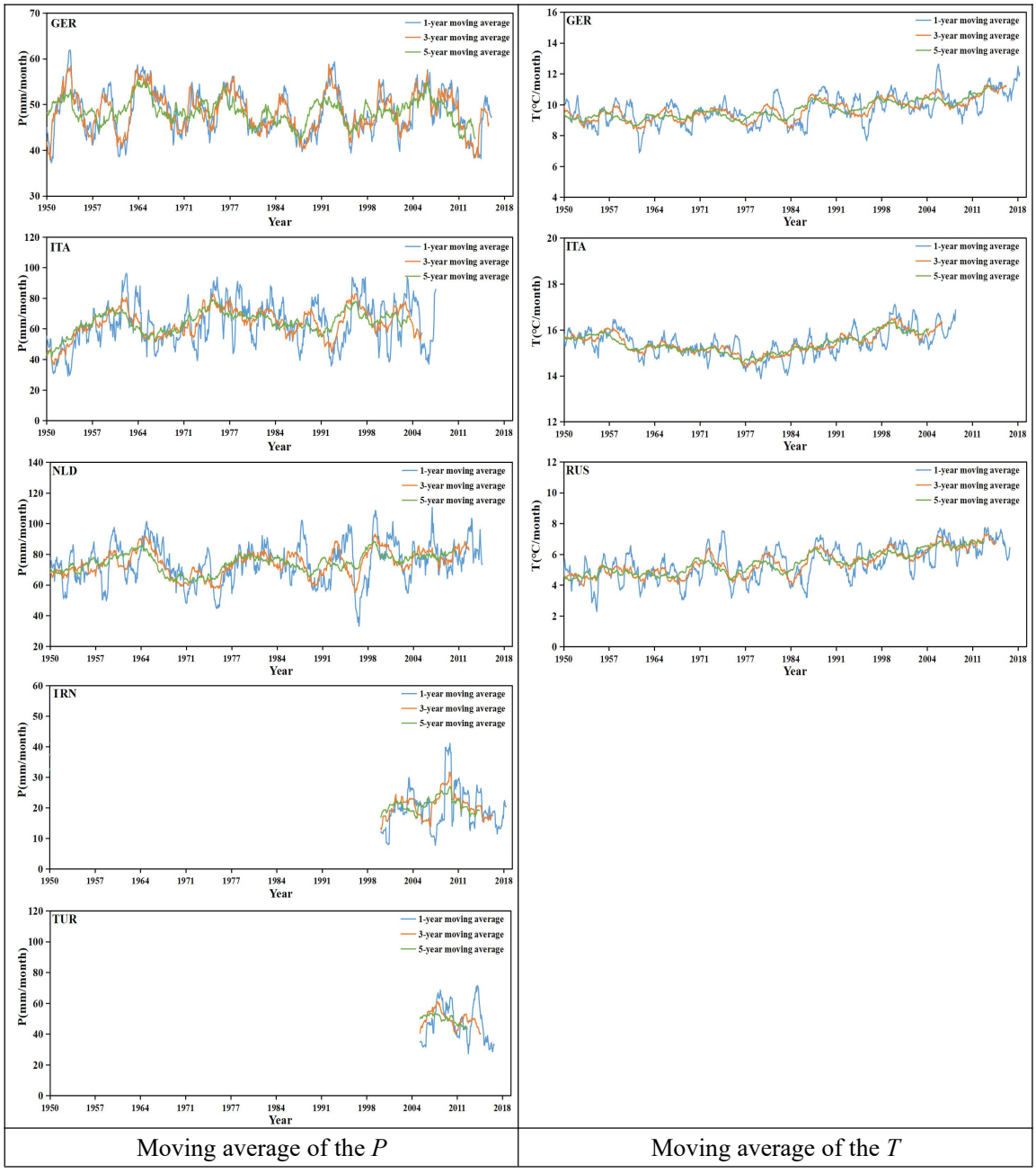

Fig.3. Time series of the climatic diurnal *P*-*T* in the major cities of the SREB in recent 60 years

The multi-year *P* (*T*) showed a decrease (increase) trend in CA, with slope K_P = -0.87 and K_T = 0.011, the values of them were 427.8 mm and 11.1 ℃. The annual *P* was the most (the least) for the TJR (KAZ), and they showed a downward trend. Amplitude of decline was biggest in TJR, the *P* and *T* was lowest of the KAZ in countries along the SREB. The *P* multi-year average was the highest in TJR and UZB, 15.0°C or so. The *P* was relatively higher and relatively lower before 1969 and after 1969 in the CA, respectively, the change of westerly wind circulation might be a key factor influencing precipitation change in the district (Chen et al. 2008). The *T* of interannual temperature change was divided into three stages that the *T* was colder in 1951-1977 and 1998-2006, and warmer in 1978-1997. Therefore, it changed from cold-wet to cold-dry in the 1970s and it showed a warm-dry trend from the late 1970s to the late 1990s, the climate change might be related to Arctic Oscillation (AO), Polar Vortex, Tibetan Plateau topography and human activities (Yao et al. 2014) in CA.

On the whole, the *P* and *T* showed an increasing trend in E, with the *P* and *T* of average annual for 727.7 mm and 9.9 ℃, respectively, the NLD had the highest *P* with 893.8 mm in the cities along the SREB. The *P*

was roughly divided into two stages: 1951-1959 (less) and 1960-2015 (more), while the *T* was divided into three stages: 1951-1987, 1988-2009 and 2010-2018. Therefore,drying and wetting alternation were obvious from cold-dry to cold-wet before 1960s to the end of 1980s. From the end of the 1980s to the first decade of the 21st century, the first decade and second decade had presented a warm-wet and col-wet trend (1951-1959: cold-dry; 1960-1987: cold-wet; 1988-2009: warm-wet; 2010-2018: cold-wet), respectively. The drop in average *T* could be caused by changes in Atlantic currents in E, there had been cases of the *T* drops caused by small changes in Atlantic currents in the past. Global warming leading to the melting of arctic glaciers and the lowering of the *T* of the Atlantic currents might be a major factor in the cooling of areas controlled by the Atlantic currents, and the *T* of global surface might not rise in the next decade (Keenlyside et al. 2008).

The *P* data of the past 19 years showed a declining trend in WA on the whole. The *P* was relatively low before 2008, while the *P* was relatively high after 2008, with an average *P* for 399.7 mm. The lack of *T* data failed to account for the phenomenon of climatic variation. Wang et al. (2018) analyzed the spatial-temporal distribution characteristics of water resources in WA, the *P* showed a slight increase and decline trend in TUR and IRN, respectively. The conclusion was contrary to that in this paper, which might be caused by the different sources of meteorological data or the shorter sequence data in this paper. The *P* was affected by the thermodynamic anomaly of the Iranian Plateau, which influenced the transport of water vapor flux in WA.

4.1.2 Seasonal variation of P-T

Dividing seasons by astronomical factors, spring in March, April and may; summer in June, July and August; autumn in September, October and November; and winter in December, January and February. According to this season, the seasonal variations of *P* and *T* were analyzed in the different districts along the line that they were significantly different (Table 4). EA: summer > autumn > spring > winter, the seasonal differences in the west of WA were mainly controlled by the circulation of water vapor in the Western Pacific Ocean, Bay of Bengal and South China Sea. In addition, the variations of complex topography (Tibetan Plateau) made the differences more obvious, it was difficult for water vapor in the lower terrain to rise and condense to form rainfall. CA: spring > winter > autumn > summer, this district was not only influenced by the Atlantic Ocean and the Arctic Ocean, but also blocked by the Tianshan Mountains. However, the *P* was scarce in this district, most of them were arid and semi-arid climate zones and the seasonal distribution difference was significantly obvious. WA: winter > spring > autumn > summer, the TUR has the highest *P* in WA and the *P* was scarce in most regions. It is mainly controlled by the subtropical high-pressure belt and restricted by the topography (Iranian Plateau), the seasons difference of *P* was obvious significantly. E: autumn > summer > winter > spring (except GER and RUS), the summer *P* was highest in GER and RUS, followed by autumn. The distribution of seasonal *P* in RUS was consistent with Xi'an in EA, but it was nearly 6 times higher than Xi'an in winter. The North Atlantic oscillation (NAO) was stronger in autumn and winter, it was more prone to extratropical cyclones, resulting in a regionally similar or slightly higher precipitation in autumn and winter than in spring and summer. As a result, the temperate marine climate showed that autumn and winter were similar to or slightly higher than spring and summer in E. The climate of the NLD was controlled not only by the perennial westerlies but also by the North Atlantic Current in WE.

The countries along the SREB had the highest *T* in summer, summer > autumn > spring > winter, the highest *T* and lowest *T* occurred in IRN and KAN in winter, respectively. The *T* difference was the most obvious in EA, it's climate was mainly controlled by the monsoon in the west of EA, the Qinghai-Tibet Plateau and the surrounding mountains strengthened the monsoon circulation system, and the *T* became lower with the higher terrain. CA belonged to a continental climate of temperate deserts and grasslands, which was influenced by the circulation of westerly circulation and other factors, resulting in significant differences in variation of *T* in different seasons. WA was a tropical desert climate that it was controlled by perennial subtropical high or low

latitude trade, prevailing downdraft, less precipitation, large evaporation, hot and dry all year-round. The climate was complicated in E, the *T* continental climate had four distinctive seasons and concentrated precipitation in CE (GER) and EE (RUS). SE (ITA) had a Mediterranean-style climate, which was controlled by the subtropical high pressure belt in summer. The water *T* of the Mediterranean was lower than that of the land causing high pressure, which strengthened the influence force of the subtropical high pressure belt, the water *T* was relatively high in winter forming low pressure and strengthening the force of the west wind. WE (NLD) belonged to the temperate maritime climate, winter has a warm current through, active extratropical cyclone, warm and humid climate.

Table 4 Seasonal of *P*-*T* in the district of SREB

District	Station	*P*				*T*			
		Spring	Summer	Autumn	Winter	Spring	Summer	Autumn	Winter
EA	Xi'an	129.2	236.0	183.0	24.0	14.8	26.1	14.2	1.9
	Lanzhou	61.6	174.5	70.9	4.9	12.0	21.9	10.3	-2.9
	Urumqi	62.0	97.3	68.1	41.5	-0.1	21.5	16.5	-8.3
CA	KAZ	51.8	56.1	39.7	44.8	5.4	21.7	5.3	-13.8
	KYG	334.8	14.2	86.3	230.8	15.1	25.9	15.6	4.5
	TJR	159.9	56.1	94.6	83.5	10.7	22.5	10.4	-1.9
	UZB	172.4	236.0	183.0	24.0	15.3	26.4	14.6	3.1
WA	IRN	79.3	21.8	41.3	93.3	18.1	30.2	19.7	5.6
	TUR	181.0	77.1	116.7	185.2			—	
EE	RUS	124.4	192.4	132.8	127.9	9.3	18.6	10.1	1.0
CE	GER	163.9	242.9	265.7	221.2			—	
WE	NLD	183.2	83.1	269.3	223.2	13.7	23.4	16.5	8.2
SE	ITA	130.8	236.9	180.6	138.3	5.8	17.7	5.2	-6.9

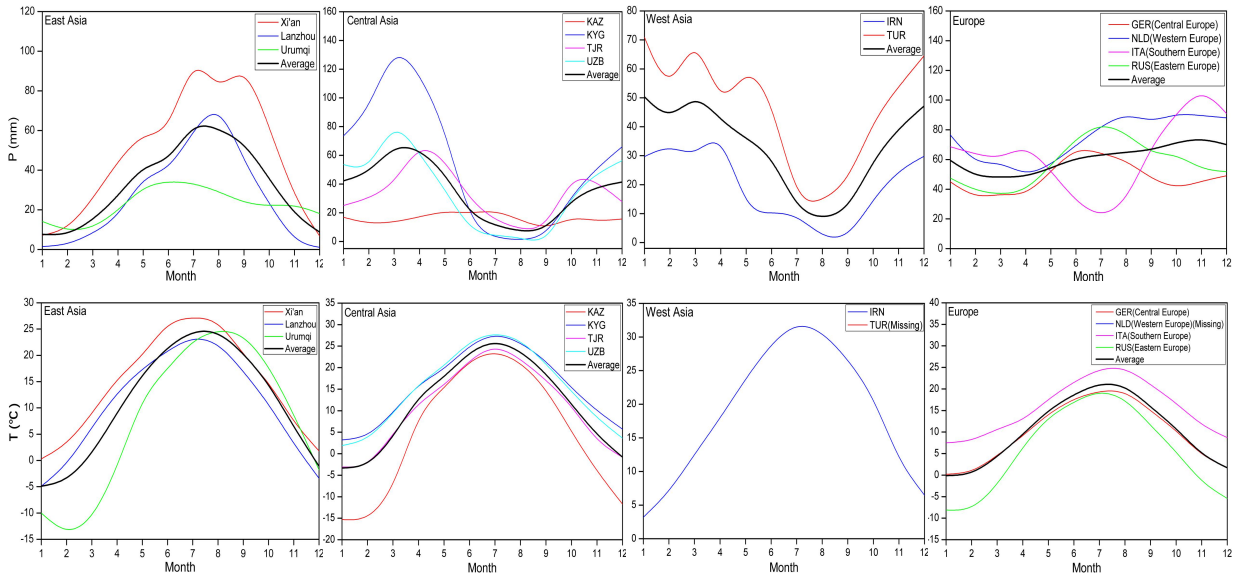

Fig.4. Morphological variation of monthly *P*-*T* in each district of the SREB

The morphological variation of annual *P* and *T* were showed in Fig. 4 in different districts of SREB. The monthly *P* in EA presented an inversely "V" shape and the high value appeared in July, with the annual average precipitation was 384.3 mm. The distribution was "V" shape (May-December), with frequent fluctuations before June, January and August were highest and lowest in WA. The average monthly *P* in TUR was 4.4 times that in IRN and that they have a significant difference. The amplitude of monthly variation was large in CA, which showed a "N" shape distribution, the average annual *P* was the highest in March, 91.2 mm. It was the least from June to September and the lowest occurred in August, only for 4.6 mm. The average annual *P* was the lowest (192.4mm) in KAZ, with significant climatic differences. The variational amplitude of monthly *P* was gentle in E, indicating that the climate was more suitable. The amplitude of variation in the latter half of

the year was larger than that in the first half of the year, the fluctuation was the most pronounced in ITA.

Although there were significant differences in monthly *P* variations in different districts due to the *P* was affected by atmospheric circulation, topography and other factors, the annual *T* variations were unimodal uniformly in different districts, with the highest in June to September. The main reason why there was a small difference in average *T* between the CA and EA was that both districts had continental climate so that the difference was not obvious. Unstable and complex European climate system lead to more frequent extreme weather events.

4.2 Variation diagnosis

The B-G algorithm was used to diagnose the variation of *P* and *T* in SREB districts after 1950, threshold value P_0 for 0.95 and the minimum segmentation scale l_0 for 25. The time series index was tested by M-K method when l_0 was less than 25, the variation diagnosis results of these districts were shown in Fig. 5. Mutation points of the *P* were not found in EA and CA during this period indicating that the annual variation of the *P* was relatively uniform and consistent with the regularity of variation trend in this period. In E, the T (statistical magnitude) reached its maximum value in 1960, P (T_{max})=0.9941 > P_0, so its sequence was divided into two periods in 1960, therefore, the mutation points was 1960 in E. The *P* increased and decreased before 2005 and after 2005 in WA, respectively, and the mutation point happened in 2003. The mutation points were detected and passed the threshold value P_0 in EA, CA and E, which occurred in 1993, 1978 and 2009, respectively. This conclusion was consistent with the results described in section 3.1.1 (Fig. 2).

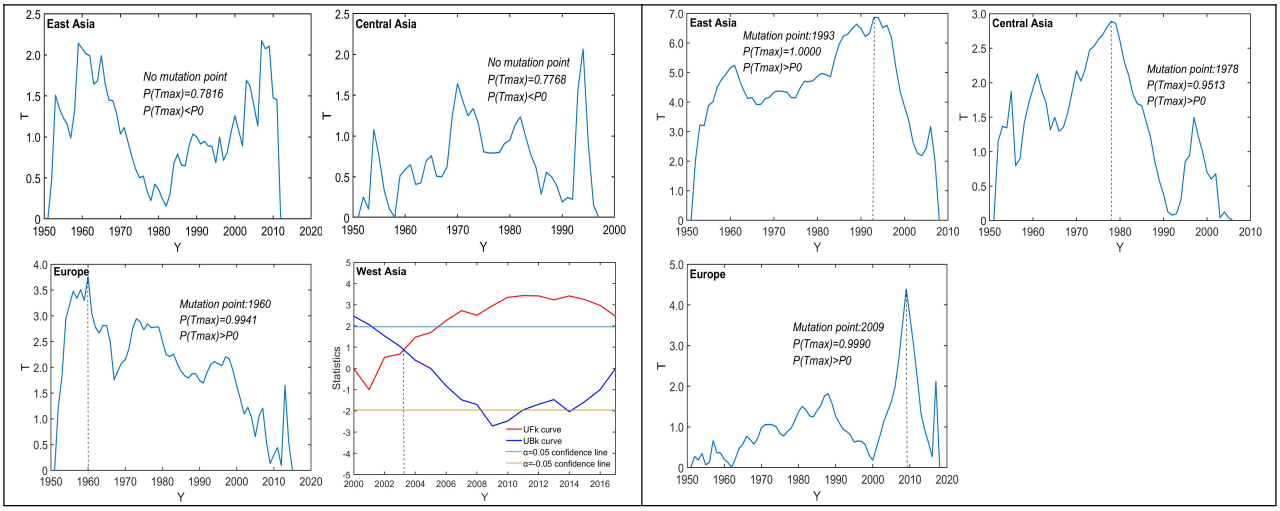

Fig.5. Variation diagnostic results of *P*-*T* in each district of the SREB (L: *P*, R: *T*)

The variation diagnosis results of cities along the BR were showed in Table 5, all cities where mutation points were detected P (T_{max}) > P_0. The mutation point of *P* weren't found in half of the cities, while the mutation point of *T* were found and passed the threshold value, they indicated that *T* was more sensitive to environmental change than *P*, the consistency of the *T* sequence was destroyed so that the global climate was gradually rising. Except for KAZ, the mutation point occurred in 1977 in CA and the amplification of *T* was obvious after 1977, while the mutation time of cities weren't synchronous along the other districts. It could be seen that the *P* increased significantly in Urumqi and KAZ in 1983, while that increased significantly in TUR and GER in the 1960s combined with the amplification variation in Table 2.

Table 5 Variation diagnostic results of *P*-*T* in the SREB

Station	*P*		*T*		Station	*P*		*T*	
	$P(T_{max})$	Mutation point	$P(T_{max})$	Mutation point		$P(T_{max})$	Mutation point	$P(T_{max})$	Mutation point
Xi'an	0.7816	—	1.0000	1993	IRN	0.9604	2002	—	
Lanzhou	0.7583	—	0.9999	1986	TUR	1.2683	1960	—	

Urumqi	0.9971	1983	1.0000	1961	RUS	0.9775	1965	1.0000	1988
KAZ	0.9892	1983	0.9998	1977	GER	0.7107	—	0.9655	2010
KYG	0.6921	—	0.9714	1979	NLD	0.9068	—	—	
TJR	0.8821	—	0.9985	1977	ITA	0.9837	1956	0.9999	1999
UZB	0.4962	—	1.0000	1977					

4.3 Spatial variation characteristic of *P*-*T*

The average annual *P* of SREB decreased spatially from west to east (Fig. 6 (Left)). Central Asia and east Asia were deeply inland, water vapor were transported far away from the ocean and the spatial distribution was from west to east, water vapor transport was more difficult with the gradual increase of the terrain so that there was less *P* in high altitude areas. The *P* of KAZ in CA was the least, at 192.1mm. The E surrounded by the north Atlantic and Mediterranean, the moisture content over the sky was rich and the necessary conditions for rainfall were sufficient so that the *P* was the largest. The annual average *P* of NLD was highest in WE, about 894.0 mm. The spatial distribution of *P* was basically the same in summer and autumn(Fig. 6b, 6c (L)), the low-value of *P* was distributed in CA and WA of SREB, but distribution of *P* was more evenly in autumn than summer. The spatial distribution of *P* was more uniform in spring than other seasons, with the largest *P* in KAZ (Fig. 6a (L)), the spatial distribution pattern of winter *P* was high in the west and low in the east in SREB (Fig. 6d (L)).

The average *T* showed a distribution pattern of high at both ends and low in the middle in SREB in recent 67 years (Fig. 6(R)), the increase of *T* was the most obvious in EA (0.33°C/10a) and the lowest in E (0.09°C/10a) (Table 2). The high *T* districts were mainly concentrated in Xi'an in WA and TJR and UZB in CA, the main reason was that the air temperature increased sharply under the control of the western Pacific subtropical high. The spatial distribution of seasonal *T* showed that the high temperature was located south of 40°N in SREB. The spatial distribution of spring and winter *T* were relatively consistent (Fig. 6a, 6d (R)), the highest *T* were found in the southwest, it mainly distributed in IRN in WA and ITA in SE and the lowest *T* were found the RUS in EE, KAZ in CA and Urumqi in EA. The high-value of summer was opposite to other seasons (Fig. 6b (R)), the high temperature occurred in IRN in WA and some countries in the surrounding CA, while the *T* in summer was relatively low in E. Distribution of the autumn *T* was similar to the spring except Urumqi and the autumn *T* in Urumqi increased in EA (Fig. 6c (R)), the phenomenon that the *T* became lower with the higher terrain was inapplicable in Xinjiang in EA and IRN in WA. The reason was that the Qinghai-Tibet Plateau and the Iranian Plateau were distributed in this district, which lead to unconventional variation in *T*.

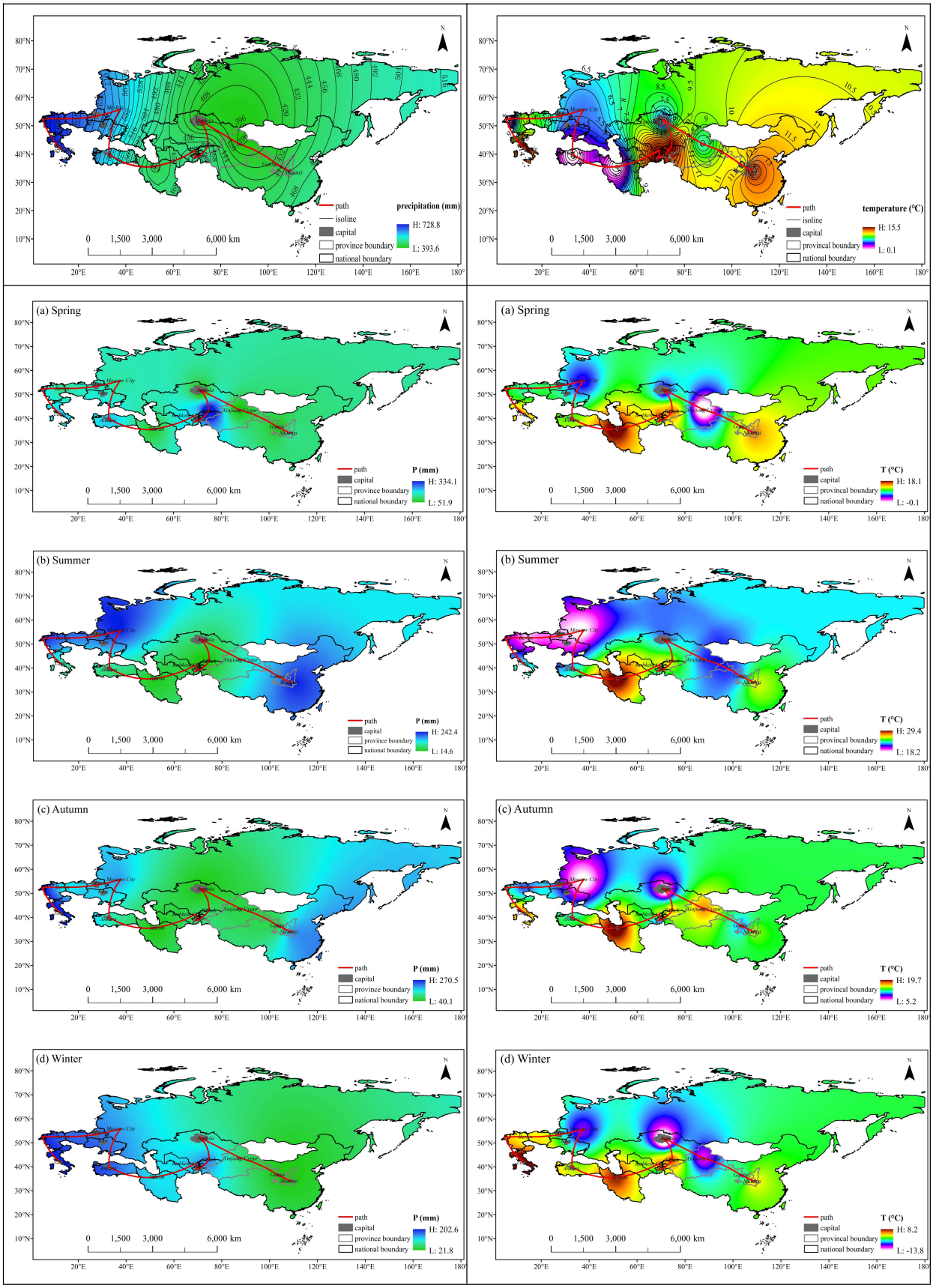

Fig.6 Spatial distribution of climate change in the SREB

4.4 Correlation characteristics of *P-T*

The relevant Pearson's matrix of 13 countries along the routes of SREB was showed in Fig. 7. The *T* data were missing for IRN and TUR in WA, it showed in # and the null background was drew with a red band (-1). The correlation of *T* (Fig. 7b) was significantly higher than that of *P* (Fig. 7a) among countries, the *T* was inversely correlated and non-significant between IRN and western China, while that between other countries was positively correlated and 2/3 of the countries were more significant (P <0.05). In Fig. 7, the correlation coefficients of *T* and *P* were concentrated at 0.4 (P < 0.05, significant) and -0.4 (not-significant), respectively, indicating that the *T* variations were more sensitive and changeable than *P* variations in various countries in recent years, the influence and interaction were inseparable between the two. The global climate becoming warming under the natural interior and exterior stress condition, air temperature increases, the increase of air *T* decreased the water holding capacity of the atmosphere and increased the probability of *P,* regional *T* variations was significantly affected by atmospheric circulation and ocean currents. The *P* in 2/5 countries were inversely correlated but non-significant, this phenomenon mainly reflected in European countries. The main reason were that snow melt in mountainous areas increased convective activity and atmospheric circulation affected water vapor transport enhancement leading to frequent extreme weather in the region under the background of global warming (Moberg & Jones 2005; Yao et al. 2014). The correlation coefficients passed the significance test (P < 0.05) only 1/8 countries, the correlation coefficient was as high as 1.00 between TUR and Lanzhou and the TUR had the highest *P* in WA. The *P* was affected by the thermal anomaly of the Iranian Plateau in WA influencing the transport of water vapor flux, the *P* variation was affected by the thermal change of the Qinghai-Tibet Plateau in northwest China, it was more favorable to form the moisture conditions of *P* in northwest China under the combined action of the two (Zhao et al. 2013).

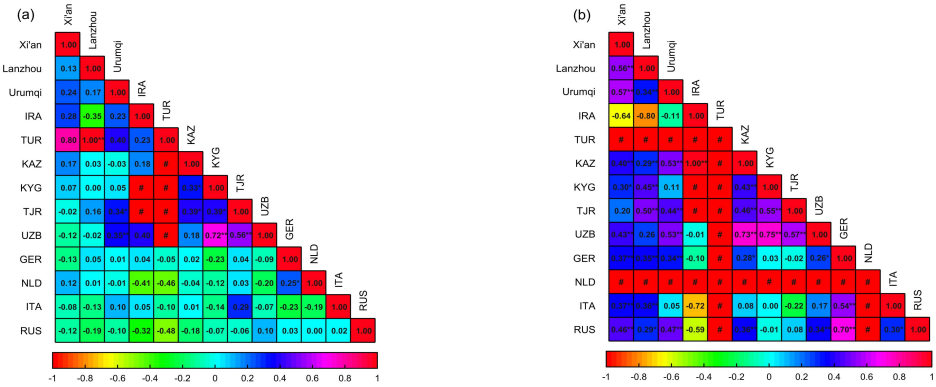

Fig.7. Pearson's correlation matrix of SREB in recent 50 years (*significant at the P < 0.05 level; **significant at the P < 0.01 level; # for a null value)

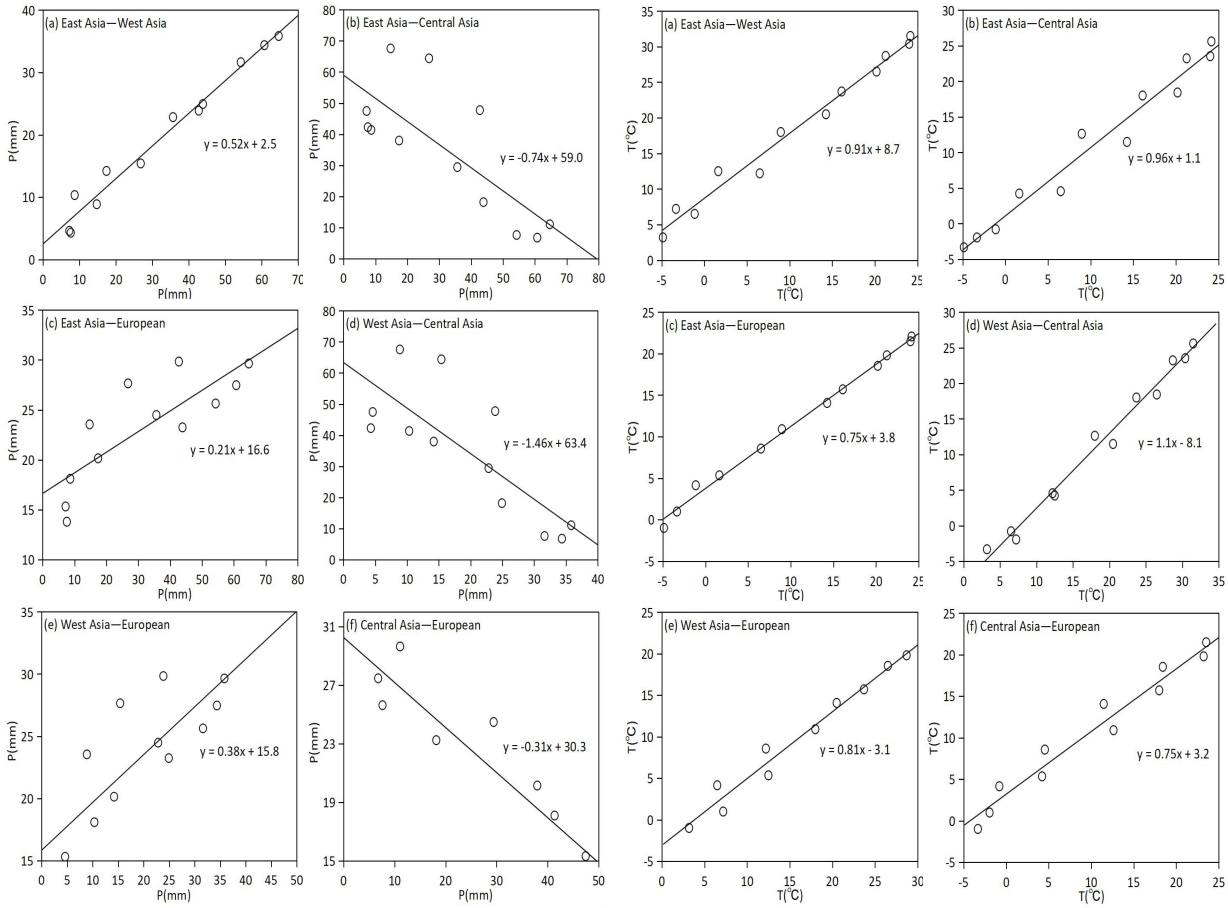

Fig.8. Correlation relationship of *P*-*T* in each district of SREB

The correlation analysis was shown in Fig. 8 between the *P* and *T* in SREB district, the *P* in CA showed an inverse correlation with EA, WA and E, while the *P* showed a positive correlation in other districts, however, there was a high-positive correlation between the *T* in all districts ($R \geqslant 0.75$). SPSS software was used to analyze the correlation among districts and it was found that there was an inverse correlation between the *P* and *T* in EA (except RUS), Xi'an in EA and KYG in CA have higher significance level ($P < 0.01$). In conclusion, the inverse correlation was better in CA, and the higher the temperature, the less the precipitation.

Table 6 was the Pearson's correlation matrix of the *P* and *T* in the study area, the *T* showed a high-positive correlation ($r > 0.98$, $P < 0.01$) in all sections of SREB, this indicated that the *T* of SREB were rising without exception under the background of global warming. The *P* in CA was high-negative correlated with EA ($R = -0.75$, $P < 0.01$) and WA ($R = -0.78$, $P < 0.01$) and it was low-negative correlated with the E ($R = -0.26$) and failed the significance test. In addition to the negative correlation above, the *P* showed a high-positive correlation and passed the significance test ($P < 0.01$) in all districts and the *P* of KAZ and TJR in CA showed a downward trend (Fig. 3), with a maximum decline for -2.62 mm/a in TJR (Tab.2).

Table 6 The Pearson's correlation matrix of *P*-*T* in each district

District	*P*				*T*				*P*-*T*
	EA	WA	CA	E	EA	WA	CA	E	
EA	1.000				1.000				-0.167
WA	0.988**	1.000			0.991**	1.000			—
CA	-0.757**	-0.789**	1.000		0.983**	0.993**	1.000		-0.392**
E	0.816**	0.804**	-0.268	1.000	0.983**	0.990**	0.984**	1.000	0.087

**significant at the $P < 0.01$ level.

The correlation equations of *P* and *T* in different districts were listed in Fig. 8, and the Formula (1) was the correlation equation after average optimization. Where, a, b, c and d represented EA, WA, CA and E

respectively.

$$P(mm)\begin{cases} b = 0.52a + 2.5 \\ c = -0.75a + 59.4 \\ d = 0.21a + 15.1 \end{cases} \qquad T(^{\circ}C)\begin{cases} b = 0.91a + 8.7 \\ c = 0.98a + 1.3 \\ d = 0.75a + 6.3 \end{cases} \tag{1}$$

In the formula, the *P* and *T* in other regions could be deduced take EA as the independent variable. Under the same conditions, the *T* increase in WA was the highest, followed by E and lowest in CA. Similarly, the *P* growth was highest in CA, second in E and lowest in WA, the change of *P* growth was completely opposite to the *T*. We can deduce the climate change of countries along the SREB through the acquisition and calculation of meteorological data in northwest China, especially those countries that lack meteorological data monitoring are more important. Establishing the correlation between different indexes and studying the similarity of climate change characteristics in different districts provide a theoretical basis for the sustainable development of SREB water resources.

5 Conclusion

(1) The *P* showed a downward trend except Urumqi in EA, the climate transformed from cold-wet to cold-dry before 1988 and showed a warm-dry trend after 1988. The warm-dry trend was related to the enhanced greenhouse effect in China. The multi-year *P* (*T*) showed a decreasing (increasing) trend in CA, the climate changed from cold-wet to cold-dry in the 1970s and it showed a warm-dry trend from the late 1970s to the late 1990s, the climate change might be related to AO, Polar Vortex, Tibetan Plateau topography and human activities in CA. The *P* and *T* showed an increasing trend in E on the whole, the climatic variation shifted from cold-dry to cold-wet in 1960-1980, and it showed a trend of warm-wet in 1980-2010 and cold-wet since 2010, with obvious alternations between drying and wetting. The decline of average *T* might be caused by changes in Atlantic currents in E.

(2) There were differences in seasonal climate caused by different atmospheric circulation characteristics and topographic conditions in different districts, there were significant differences in seasonal *P* and the *T* showed summer > autumn > spring > winter in different districts. The rest districts were controlled by a climate system, but the E was controlled by the multiple climate systems that lead to frequent extreme weather events. Although the variation of monthly *P* was greatly difference influenced by atmospheric circulation and topography, the annual variations of *T* was uniformly unimodal in different districts, with the highest in June to September.

(3) Mutation points of the *P* were not found in EA and CA during this period indicating that the annual variation of the *P* was relatively uniform in this period. The mutation points of variation was detected in E in 1960. The mutation points were detected and passed the threshold value P_0 in EA, CA and E, which occurred in 1993, 1978 and 2009, respectively, this conclusion was consistent with the description of accumulated anomalies in the different districts. The *T* was more sensitive to environmental change than *P*, the consistency of the *T* sequence was destroyed so that the global climate was gradually rising.

(4) The average *P* of SREB decreased from west to east in space and there was abundant *P* in E in recent 67 years. The average *T* showed a distribution pattern of high at both ends and low in the middle, the high *T* was mainly concentrated in Xi'an in EA, TJR and UZB in CA, the main reason was that the air temperature increased sharply under the control of the western Pacific subtropical high. Through the analysis of the Pearson coefficient between *T* and *P*, it was found that the *T* variations were more sensitive and changeable than *P* variations in various countries in recent years, the influence and interaction were inseparable between the two.

(5) This study provided an in-depth and comprehensive analysis of climatic variation in the SREB district, which could be regarded as a beneficial supplement in the research field of climatic variation. The research of

climatic variation on other scales also should be actively carried out adapting to different needs so as to enrich the think-tank of decision-relevant to climate change.

6 Outlook and forecast

The cities along SREB had less *P* and lower *T i*n general. The water resources problems are complex and diverse of countries along the BR, how to quantitatively solve the water problems of BR needs to be combined with various countries to enrich water control experience and highly ideological strategy, so as to solve the water problems from the root and build the value concept of “clear water and green mountains”. We should strive to solve the problem of ownership of water resources of each country, avoid disputes over water resources, tap the potential of water resources cooperation as far as possible, and achieve the structure of “low conflict-high cooperation” among each country.

Climate change is a major global challenge facing the world in the new era, it has a profound impact on the ecology, economy, society and human survival and development. How to actively carry out climate cooperation and build a green community with a shared future among countries along the BR has become an important topic in the international climate governance system. Although countries have formed effective cooperation models in other aspects, it is difficult to advance on climate change, the main reason is the lack of legal binding principles related to climate change, together with the gradual and flexible effect of climate change on regional cooperation to actually deal with climate change. All countries should follow the vision of a community with a shared future, actively respond to climate cooperation and ecological civilization construction, and establish a reasonable and effective climate cooperation mechanism to drive and promote regional climate cooperation combined with local climate characteristics, so as to ensure the sustainable development of all countries and achieve the strategic goal of SREB in a real sense.

Acknowledge

This work was supported by the National Key R&D Program of China (2016YFC0401408) and the National Natural Science Foundation of China (51679188, 51979221). the authors acknowledge the financial support above mentioned and valuable comments of the students in the teaching and research section.

Data availability statement

All data that support the findings of this study are included within the article (and any supplementary information files).

References

Bai Y Q, Wang J L, Wang Y J, et al. Spatio-temporal distribution of drought in the Belt and Road Area during 1998-2015 based on TRMM precipitation data[J]. Journal of Resources and Ecology, 2017, 8(6): 559-570.

Chen F H, Yu Z C, Yang M L, et al. Holocene moisture evolution in arid central Asia and its out-of-phase relationship with Asian monsoon history[J]. Quaternary Science Reviews, 2008, 27 (3): 351-364.

Dong T Y, Dong W J, Guo Y, et al. Future temperature changes over the critical Belt and Road region based on CMIP5 models[J]. Advances in Climate Change Research, 2018, 9(1): 57-65.

Han T T, Chen H P, Hao X, et al. Projected changes in temperature and precipitation extremes over the Silk Road Economic Belt regions by the Coupled Model Intercomparison Project Phase 5 multi-model ensembles[J]. International Journal of Climatology, 2018, 38(11): 4077-4091.

Jiang Lingyan. Analysis of water resource characteristics and supporting capacity of “Belt and Road”[J]. Jiangxi Agriculture, 2019(02): 105.

Keenlyside N S, Latif M, Jungclaus J, et al. Advancing decadal-scale climate prediction in the North Atlantic sector[J]. Nature, 2008, 453 (7191): 84-88.

Li Mingliang, Li Yuanyuan, Hou Jie, Xiao Peng, Gao Yaqi. Opportunities and challenges for water resources cooperation under the “Belt and Road” Initiative[J]. China Water Resources, 2018(23): 4-6+3.

Li Sha, Shu Hong, Dong Lin. Research and realization of Kriging interpolation based on spatial-temporal variogram[J]. Computer Engineering and Applications, 2011, 47(23): 25-26+38.

Lin Li. The Analysis of integrated water resources management by the Five Central Asian Countries on the New Silk Road Economic Zone[J]. West Forum, 2015, 25(04): 77-83.

Ma Lan, Huang Shengzhi, Huang Qiang, Xue Qi, Li Pei, Liu Saiyan. Causes Analyzing of the Change of Rainfall and Rainfall Erosivity in Weihe River Basin[J]. Journal of Soil and Water Conservation, 2018, 32(01): 174-181+189.

Moberg A, Jones P D. Trends in indices for extremes in daily tem-perature and precipitation in central and western Europe, 1901-99[J]. International Journal of Climatology, 2005, 25: 1149-1171.

OECD. Water and Cities:Ensuring Sustainable Futures, OECD Studies on Water[R]. OECD Publishing, Paris, 2015.

Pei Yixuan. The fundamental principle and application of sliding average method[J]. Journal of Gun Launch & Control, 2001(01): 21-23.

Peng D D, Zhou T J, Zhang L X, et al. Human Contribution to the Increasing Summer Precipitation in Central Asia from 1961 to 2013[J]. Journal of Climate, 2018, 31(19): 8005-8021.

Qi Qinghua, Cai Rongshuo. The Climate Changes of Marine Environment and Storm Risk on the 21st Century Maritime Silk Road[J]. Ocean Development and Management, 2017, 34(05): 67-75.

Qi Qinghua, Cai Rongshuo. Spatio-Temporal Change of Sea Surface Temperature Anomalies in Seas of 21st Century Maritime Silk Road and Its Net Correlation to Climate Variability[J]. Ocean Development and Management, 2017, 34(04) :41-49.

Qiang Anfeng, Wei Jiahua, Xie Hongwei. Trend Analysis of Temperature and Precipitation in Sanjiangyuan Region of Qinghai Province[J]. Water Resources and Power, 2018, 36(02): 10-14.

Shi Yafeng, Shen Yongping, Li Dongliang, et al. Discussion on the present climate change from warm-day to warm wet in Northwest China[J]. Quaternary Sciences, 2003 (02): 152-164.

Tan Xue, SHI Lei, WANG Xuejun, XU Ke, MA Zhong, ZHANG Xiangshu. Regional water efficiency evaluation and deconstruction analysis of the New Silk Road Economic Belt[J]. Journal of Arid Land Resources and Environment, 2016, 30(01): 1-6.

Wang H J, Zuo Q T; Hao L G; Han C H; Ma J X. Anglysis of spatial-temporal characteristics and spatial equilibrium of precipitation in West Asia area ofBelt and Road[J]. Water Resources Protection, 2018, 34 (4): 35-41.

Wang Lina, Chen Xiaohong, Li Yuean, Lin Kairong. Heuristic segmentation method for change-point analysis of hydrological time series[J]. Yangtze River, 2009, 40(09): 15-17+106.

Xu Meiling, Xing Tong, Han Min. Spatial-temporal data interpolation based on spatial-temporal Kriging method[J]. Acta Automatica Sinica, 2019, 44(X): 1-8.

Xu Xinliang, Wang Liang, Cai Hongyan. Spatio-temporal characteristics of climate change in the Silk Road Economic Belt[J]. Resources Science, 2016,38(09):1742-1753.

Yan Long, Ma Jing, Li Dili, Deng Wei. International comparison of water resources utilization efficiency in the core area of the Silk Road Economic Belt[J]. Journal of China Institute of Water Resources and Hydropower Research, 2018, 6(06): 521-527+535.

Yang Jingwen, Sun Jilin, Reiner S. Trends in Frequency and Intensity of Extreme Precipitation at Four German Stations[J]. Periodical of Ocean University of China, 2010, 40 (S1): 23-30.

Yang Yanzhao, Feng Zhiming, Sun Tong, Tang Feng. Water resources endowment and exploitation and utilization of countries along the Belt and Road[J]. Journal of Natural Resources, 2019, 34(06): 1146-1156.

Yao Junqiang, Liu Zhihui, YangQing, et al.Temperature variability and its possible causes in the typical basins of the arid Central Asia in recent 130 years[J]. Acta Geographica Sinica, 2014, 69 (3): 291-302.

Zhang Jie. Assessment report on China's peripheral security situation (2015): "Belt and Road" and peripheral strategy[M].World Affairs, 2015.

Zhao Yong, Yang Qing, Huang Anning, Qian Yongpu. Relationships between the anomalies of surface sensible heat in the Tibetan Plateau and Iran Plateau and summertime precipitation in North Xinjiang[J]. Acta Meteorologica Sinca, 2013, 71 (04): 660-667.

Zhao Z C, Xu Y. Detection and projection of temperature change in East Asia for the 20th and 21st centuries [J]. Review of World Resources (USA), 2003, 9: 223-234.

Zhen Chongwei, Gao Chengzhi, Gao Yue. Climate feature and long term trend analysis of wave energy resource of 21st Century Maritime Silk Road[J]. Acta Energiae Solaris Sinica, 2019, 40(06): 1487-1493.

Zhou T J, Sun N, Zhang W X, et al. When and how will the Millennium Silk Road witness 1.5 °C and 2 °C warmer worlds?[J]. Atmospheric and Oceanic Science Letters, 2018, 11(02): 180-188.

Zuo Qiting, Han Chunhui, Hao Lingang, Wang Haojie, Ma Junxia. The main route and water resource areas of the Belt and Road Initiative[J]. Resources Science, 2018, 40(05): 1006-1015.

Zuo Qiting, Han Chunhui, Ma Junxia, Liu jing. Water resources characteristics and supporting capacity for “the Belt and Road” in China mainland[J]. Journal of Hydraulic Engineering, 2017, 48(06): 631-39.

Zuo Qiting, Hao Lingang, Liu Jianhua, Ma Junxia, Wang Haojie, Han Chunhui. Characteristics of water resources in “Belt and Road” district and its framework of water security system[J]. Water Resources Protection, 2018, 34(04): 16-21+28.

Zuo Qiting, Hao Lingang, Ma Junxia, Han Chunhui. “Belt and Road” water problem in regionalization and reflections on drawing lessons from China's water management experiences[J]. Journal of Irrigation and Drainage, 2018, 37(01): 1-7.